Laser-Induced Iodine Fluorescence Technique for Quantitative Measurement in a Nonreacting Supersonic Combustor

D. G. Fletcher* and J. C. McDaniel†
University of Virginia, Charlottesville, Virginia

A nonintrusive optical technique, laser-induced iodine fluorescence (LIIF), is demonstrated in the quantitative study of the compressible flowfield in a steady, nonreacting supersonic combustor. Measurements of density, temperature, and velocity were made with the calibrated technique for two combustor operating conditions. Measurements were first conducted in the supersonic flow over a rearward-facing step for comparison with calculated pressure profiles. The second operating condition was staged, transverse injection behind a rearward-facing step at an injection dynamic pressure ratio of 1.20. These experimental results demonstrate the capability of the technique for making accurate, spatially resolved measurements of gasdynamic variables in the complex supersonic flowfield. Complete data sets to be generated with this technique will be used to validate computational fluid dynamic (CFD) codes for supersonic combustor flowfields, prior to the inclusion of chemical reaction.

Introduction

PROPOSED supersonic combustor configurations engender complex, compressible flowfields that present a considerable computational challenge, even without chemical reaction. The mixing of high-speed, compressible gas streams injected transversely into a supersonic freestream behind a rearward-facing step is highly three-dimensional and dominated by shock waves and shock-wave/boundary-layer interactions. However, in order to design airbreathing propulsion systems for hypersonic flight, computational fluid dynamic (CFD) codes must be developed to model these flowfields. The codes will extend combustor studies beyond the capability of ground-test facilities[1] and ultimately provide insight into the fundamental processes governing ignition and flameholding.

Confidence in these CFD codes must be developed before their application, necessitating the parallel experimental investigation of supersonic combustion flowfields, first without chemical reaction. The large property gradients in these supersonic flowfields require the use of a nonintrusive, optical measurement technique with excellent spatial resolution. Unified optical techniques are preferable for compressible flowfield diagnosis because they provide the measurement of more than one gasdynamic variable simultaneously.[2,3] Laser-induced iodine fluorescence (LIIF) has been demonstrated as a qualitative tool for flow visualization[4,5] and is herein demonstrated as a quantitative, unified optical technique for spatially-resolved measurements. Both qualitative and quantitative LIIF techniques use iodine as a tracer molecule, seeded into air. Molecular iodine has a dense visible absorption spectrum and fluoresces strongly in the visible for convenient signal collection. In addition, iodine molecules are not subject to macroscopic particle lag in regions of large velocity gradients encountered in supersonic flowfields.

Simultaneous LIIF measurements of density, temperature, and velocity in a steady, nonreacting supersonic-combustor flowfield are presented in this paper. Visualization studies previously conducted in the flowfield using LIIF[6,7] were used to select the measurement locations and provide a coarse check on the results. These measurements establish the capability of the unified LIIF technique for quantitative measurement of gasdynamic variables with sufficient spatial resolution to fully characterize the flowfield. Complete data sets will be obtained with this technique for detailed, pointwise validation of the three-dimensional CFD solution for the flowfield.[7,8]

Presented as Paper 87-0087 at the AIAA 25th Aerospace Sciences Meeting, Reno, NV, Jan. 12–15, 1987; received July 9, 1987; revision received May 6, 1988.

*Graduate Research Assistant, Department of Mechanical and Aerospace Engineering. Student Member AIAA.

†Assistant Professor, Department of Mechanical and Aerospace Engineering. Member AIAA.

Experiment

LIIF

Quantitative measurements using LIIF have been reported for density,[9] velocity,[10–12] pressure,[13–15] and temperature[16] in compressible flowfields. A narrow-bandwidth, tunable dye laser, or an argon laser with an intracavity etalon, is used to selectively excite iodine transitions. The resulting broadband fluorescence signal is collected using phase-sensitive detection. In contrast with qualitative LIIF experiments, the laser beam is focused very tightly and, using small-aperture collection optics, a probe volume on the order of 0.001 mm^3 is obtained. Such high spatial resolution is absolutely necessary for pointwise measurements in large-gradient, supersonic flowfields. By scanning a dye laser across specially selected iodine absorption lines, measurements of density, temperature, and velocity in a steady flowfield are combined into a single (unified) nonintrusive technique. Figure 1 demonstrates briefly how the technique is applied. The broader spectrum (dotted line) in this figure is fluorescence collected from a point in the combustor test section. The more narrow spectrum (dashed line) is fluorescence collected from a low-pressure iodine static cell. The dye laser scans a 30-GHz region of the iodine absorption spectrum containing two adjacent transitions chosen to give maximum sensitivity to the flowfield properties of interest. Line-center signal variation resulting from narrow-bandwidth excitation of the stronger transition is inversely proportional to collisional quenching and broadening. For a uniformly seeded flowfield, this reduces to an inverse dependence on total number density. Density profiles are normalized to a value at a known reference point in the flowfield to produce absolute density measurements. The ratio of the line-center signal magnitude of the weaker transition to the stronger transition yields the ratio of Boltzmann population fractions of the two iodine transitions, from which the absolute temperature is obtained. This temperature measurement technique has been calibrated in the known flowfield of a Laval nozzle,[16] with an uncertainty of $\pm 2\%$. Once the density and temperature are measured, the local static pressure is calculated from the ideal-gas equation of state. Simultaneous excitation of

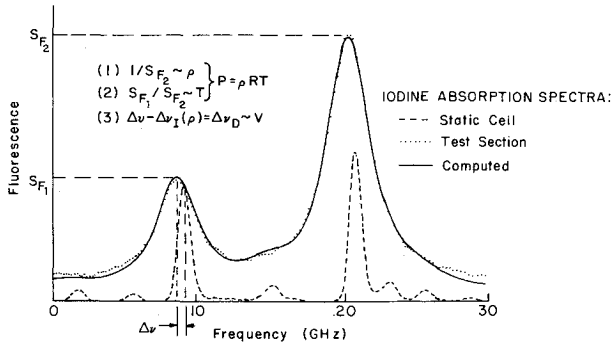

Fig. 1 Summary of the spectral line-center relationships to gasdynamic variables for the calibrated LIIF optical technique.

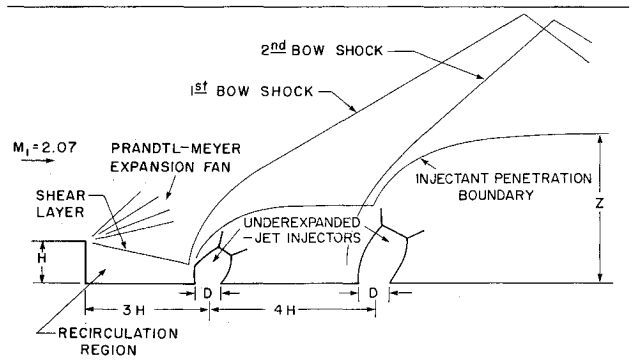

Fig. 2 Staged, transverse injection behind rearward-facing step in nonreacting supersonic combustor.

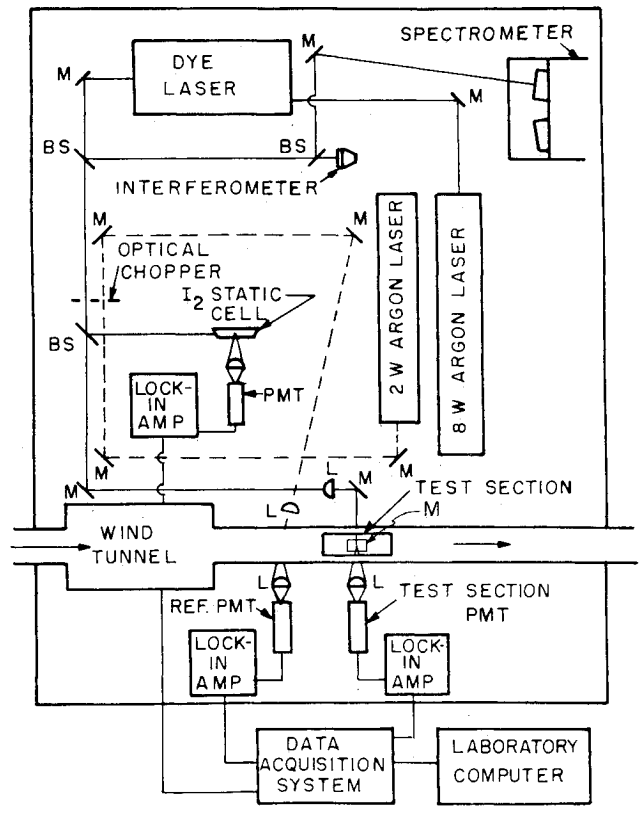

Fig. 3 Experimental configuration of the LIIF optical technique (M= mirror, L=lens, BS=beamsplitter).

iodine in the static cell provides a reference fluorescence signal for determining velocity from the frequency shift between the absorption peaks. In Fig. 1, the shift is to lower frequency, indicating a velocity component direction opposing laser beam propagation. The transitions are also frequency-shifted due to collisions, a phenomenon termed the impact shift.[17] The thermodynamic dependence of the impact shift of iodine in air was determined in a calibration experiment. With this dependence known, measured density is used to calculate the impact shift contribution at each location. This impact shift is subtracted from the measured total frequency shift, and the remaining Doppler shift yields the velocity component in the laser beam direction. Uncertainty in velocity measurement is due to inaccuracy in determining line-center locations and uncertainty in the calculated impact shift. At present, this velocity uncertainty is estimated to be less than $\pm 5\%$ over the range of velocities reported in this paper. Also shown in Fig. 1 is the computed fluorescence spectrum (solid line) calculated using the measured thermodynamic properties in order to provide a consistency check on the results deduced from measured line-center values alone.

Flowfield

The combustor test section was configured with staged, transverse injectors located behind a rearward-facing step. A sketch of the flowfield is presented in Fig. 2. A two-dimensional Laval nozzle provides a shock-free Mach 2.07 test section inlet freestream with $p = 31.4$ kPa and $T = 161$ K at nominal stagnation conditions of 274 kPa and 299 K. As shown in Fig. 2, the flowfield accelerates and turns past the step through a centered Prandtl-Meyer expansion fan. The rearward-facing step of 3.18-mm height H is 15% of the total combustor duct height and promotes gaseous injectant penetration and recirculation. The injectors have a diameter D of 1.98 mm, or $0.624H$ and are located at $3H$ and $7H$ downstream of the step. (Visualization studies of a similar configuration with the first injector located $4H$ behind the step did not detect a significant amount of injectant in the recirculation region behind the step.[6] Moving the injectors $1H$ upstream allows the injected gas to reach this zone, as verified by recent visualization studies.[7]) The underexpanded jet injectors exhibit barrel shocks and Mach disks that are deflected downstream by the supersonic crossflow. Also indicated in Fig. 2 are the injectant penetration boundary and injector bow shock locations determined from LIIF visualization photographs.[7]

Optical Configuration

The optical setup for the quantitative LIIF study is shown in Fig. 3. An 18-W argon laser, tuned to the 488-nm line, pumps a Spectra-Physics model 380A ring dye laser. Coumarin 540 dye is used in the ring laser because of its high gain at the iodine transition wavelength (543 nm) and its relative stability. Dye laser output power is monitored by a photodetector located within the ring cavity. A portion of the dye laser beam is sent to a spectrometer for coarse laser frequency determination and to a scanning interferometer for monitoring the laser mode during the 30-GHz scan. The beam is then chopped, and 8% is sent to an iodine static cell for precise frequency determination and reference in the velocity measurement. A micrometer-driven translation system (not shown in Fig. 3) is located beneath the tunnel and carries a lens and mirror to focus and redirect the beam vertically into the tunnel. A collection lens and photomultiplier tube, also mounted on the translation stage, translates with the laser beam and collects fluorescence emitted normal to the laser beam. Two filters (a multilayer reflective and a long-pass absorbing) at the front of the tube provide discrimination against the elastic scattering at the laser wavelength while transmitting the red-shifted fluorescence. Coated, optical-grade fused silica windows allow the laser beam to enter and leave the combustor test section with minimal reflection. The intersection of the 80-μm-diam laser beam and 200-μm-diam collection aperture, with unit magnification imaging, produces a measurement volume of 0.001

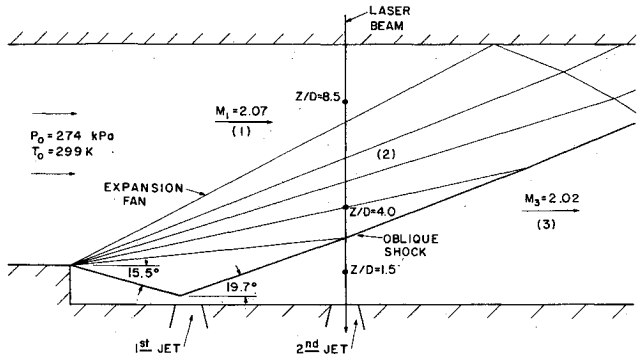

Fig. 4 Two-dimensional, method-of-characteristics solution for flow over the rearward-facing step (no injection).

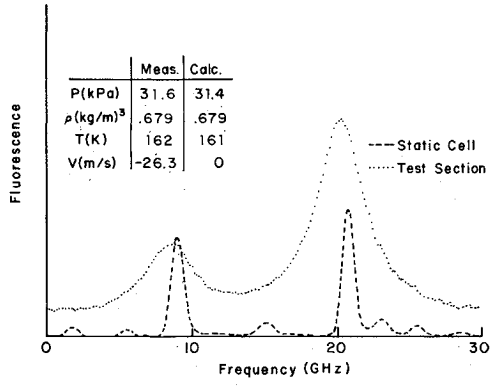

Fig. 5 Test section and static cell fluorescence spectra measured in the freestream (region 1) at the reference point ($Z/D = 8.5$).

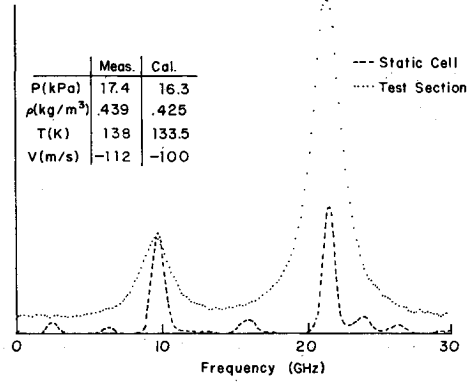

Fig. 6 Test section and static cell fluorescence spectra measured in the expansion fan (region 2) at $Z/D = 4.0$.

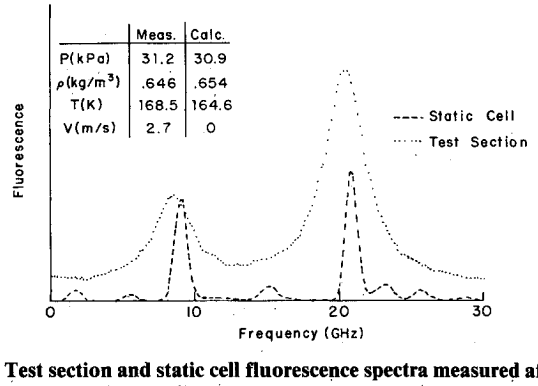

Fig. 7 Test section and static cell fluorescence spectra measured after the oblique shock (region 3) at $Z/D = 1.5$.

mm³. This high spatial resolution provides more than 10 discrete measurement locations across the 1.98-mm-diam injector orifice. Data acquisition is microcomputer-controlled and is synchronized with the computer-initiated dye laser scan once the translation stage is in position. A stationary reference photomultiplier tube, located upstream of the combustor, monitors the signal from an iodine transition excited by the broadband 514.5-nm output of a 2-W argon laser in order to provide a record of iodine seeding-fraction variation during the experiments. (Iodine is seeded into the flowfield in a room-temperature stagnation chamber that does not reach thermodynamic equilibrium during the experiment because of coupled heat- and mass-transfer effects.[15]) Spectra consisting of 600 points are acquired at each measurement location, are three-point averaged, and are then fit by quadratic polynomials to locate transition line centers. Once the line centers are located, density and temperature are determined from line-center magnitudes and velocity from the line-center frequency shift, as described previously.

Results and Discussion

Flowfield without Injection

The first experiment was conducted in the test section without transverse injection. A schematic representation of this flowfield is presented in Fig. 4. The 15.5-deg flow-turning angle through the expansion fan and the oblique shock location were obtained from a planar fluorescence photograph.[7] The flow property variation in the expansion fan (region 2 in Fig. 4) and the interaction of the expansion fan and the oblique shock were calculated using the two-dimensional method of characteristics. Measurements were made across the test section along the centerline of the second injector. Representative fluorescence spectra at the three measurement locations shown by the dots in Fig. 4 are presented in Figs. 5-7. Flow properties obtained from the fluorescence spectra are tabulated on each figure and compared with the method-of-characteristics solution.

The spectrum in Fig. 5 corresponds to the Mach 2.07 freestream conditions of 31.4 kPa and 161 K computed from the isentropic relations and the stagnation conditions given in Fig. 4. Density measurements for the entire data set were normalized to this freestream reference point. The measured freestream temperature agrees very well with the computed value, as does the pressure value derived from the ideal-gas equation of state. However, a small vertical velocity component was measured, in contrast to the assumption of uniform horizontal velocity in region 1 of Fig. 4 used to initiate the method-of-characteristics solution.

In Fig. 6, the density inside the expansion fan (region 2 of Fig. 4) is decreased from the freestream value, as indicated by the increased line-center signal of the stronger transition. A decrease in the frequency shift between the static cell and test section, compared to that of Fig. 5, is due to the reduced density, since the impact shift is large compared to the Doppler shift in these two figures. The smoothness of the scan and the sharply peaked line-center values serve to illustrate the high signal-to-noise ratio available from the measured flowfield fluorescence. The measured density is 3% higher than the value calculated by the method-of-characteristics solution, and the measured temperature is 3% higher than the calculated value. The static pressure derived from the ideal-gas equation of state is, therefore, 6% higher than the calculated value. The strong negative vertical velocity component measured at this location is due to the turning of the flow by the expansion fan.

The fluorescence spectrum obtained at the data point located behind the oblique shock (region 3 of Fig. 4) is shown in Fig. 7. The increases in temperature and density from the conditions of Fig. 6 are due to the oblique shock compression. At this location, the density measured is lower than the value from the method-of-characteristics solution by 1%. The measured temperature is 2% higher than that predicted by the

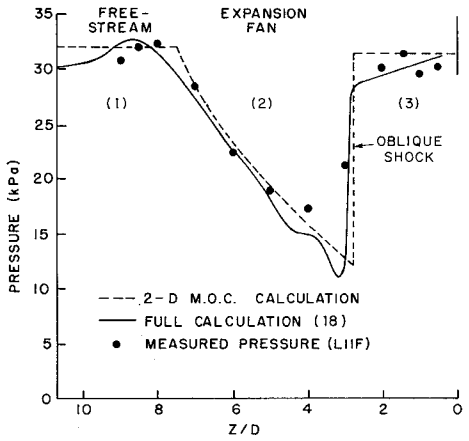

Fig. 8 Comparison of measured and calculated pressure distributions for flow over the rearward-facing step (no injection).

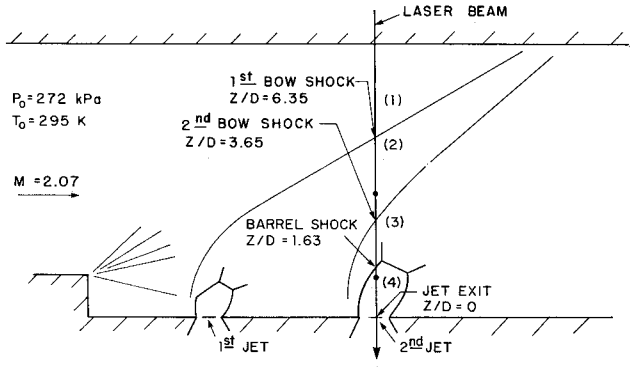

Fig. 9 Flowfield features and measurement locations for staged, transverse injection behind a rearward-facing step at $\bar{q}=1.20$.

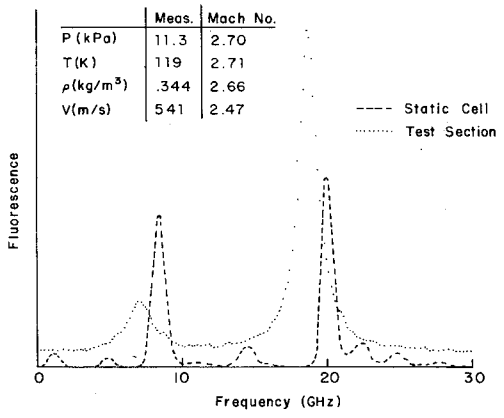

Fig. 10 Test section and static cell fluorescence spectra measured in the isentropic core of the underexpanded-jet injector (region 4) at $Z/D=1.5$ for staged injection with $\bar{q}=1.20$.

calculation. This results in a pressure value derived from the ideal-gas equation of state, which agrees to within 1% of the calculated value. The measured vertical velocity component is essentially zero, as expected in order for the flow to leave the oblique shock nearly parallel to the bottom wall.

A pressure profile, calculated from the measured density and temperature at each data-point location, is shown in Fig. 8. The method-of-characteristics solution for pressure (dashed line) and values of pressure from the computational solution of the full three-dimensional Navier-Stokes equations for the flowfield[18] are also presented in Fig. 8. The decrease in pressure from the freestream value through the expansion fan is shown, as well as the recompression across the oblique

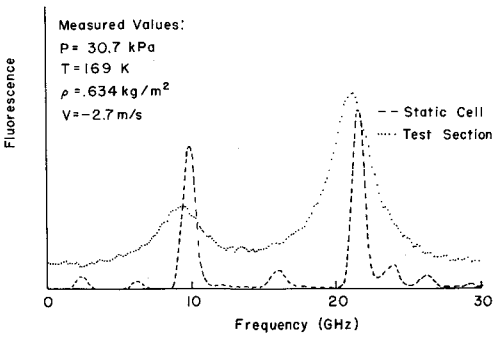

Fig. 11 Test section and static cell fluorescence spectra measured after the second injector bow shock (region 2) at $Z/D=4.0$ for staged injection with $\bar{q}=1.20$.

shock. The agreement between the full solution, the method-of-characteristics solution, and the measured values is seen to be quite good.

Flowfield with Injection

A schematic of the flowfield with staged injection at an injector-to-freestream dynamic pressure ratio $\bar{q}$ of 1.20 is shown in Fig. 9. Shock locations at the measurement profile along the second jet centerline were obtained from the visualization studies[7] and serve to delineate four distinct regions within the flowfield. Because of larger gradients in the isentropic jet core of region 4, a finer experimental grid was employed in this region.

Fluorescence spectra measured at the locations of the two dots in regions 4 and 2 of Fig. 9 are shown in Figs. 10 and 11, respectively. The fluorescence spectrum in Fig. 10 is very sharp due to the low density and temperature in the underexpanded-jet core and is strongly shifted to lower frequency because of the large vertical velocity component opposing the laser beam direction. By forming the ratio of the measured density to the injector stagnation density, a Mach number of 2.66 is obtained from the isentropic relations. Comparing this value with a Mach number of 2.71 obtained in a similar fashion using the measured temperature shows that, for the isentropic conditions in the jet core, the measured density and temperature at this location are consistent. A Mach number of 2.47, obtained from the measured temperature and vertical velocity component, is less than the aforementioned values, indicating a significant horizontal velocity component at this point.

Figure 11 shows the spectrum at the second location, in region 2. The measured velocity component in the laser beam direction is nearly zero, and the density, temperature, and pressure are close to the freestream conditions after expansion and then recompression by the first bow shock.

Distributions of pressure, temperature, and velocity component along this vertical profile are presented in Figs. 12–14. Discontinuities in the plotted data on each figure correlate well with the shock locations measured from the fluorescence photograph, with pressure and temperature increasing in the flow direction across each shock wave. The experimental uncertainty of the thermodynamic variables along this profile is less than ±5%. Although the jet was initially assumed to be sonic, a comparison of the measured pressure and temperature at the jet exit with the stagnation conditions indicates an exit Mach number of about 1.4. Using this measured Mach number and static pressure, a value of the injector-to-freestream dynamic pressure ratio $\bar{q}$ of 1.20 is obtained. However, measurements at the jet exit plane were subject to a much higher background level, due to wall scattering, than data points in the flowfield. Consequently, the measured pressure and temperature and deduced Mach number at the jet exit are subject to greater uncertainty. A velocity measurement at the jet exit point could not be made in this experiment due to this wall scattering.

Future experiments will employ a different signal collection

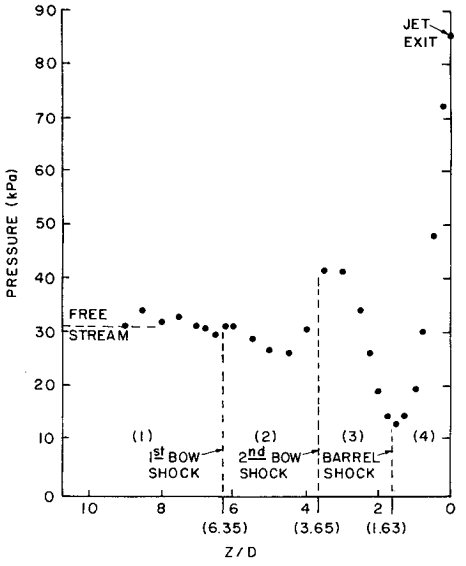

Fig. 12 Measured pressure distribution along second injector centerline for staged injection with $\bar{q} = 1.20$.

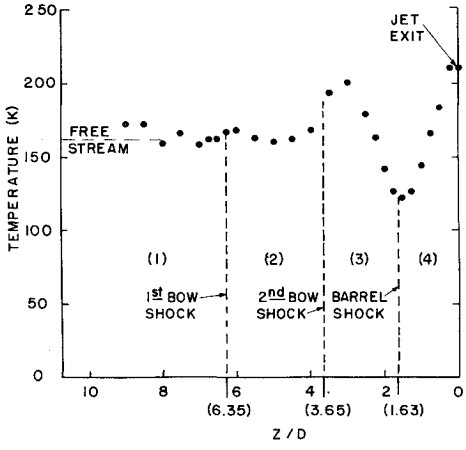

Fig. 13 Measured temperature distribution along second injector centerline for staged injection with $\bar{q} = 1.20$.

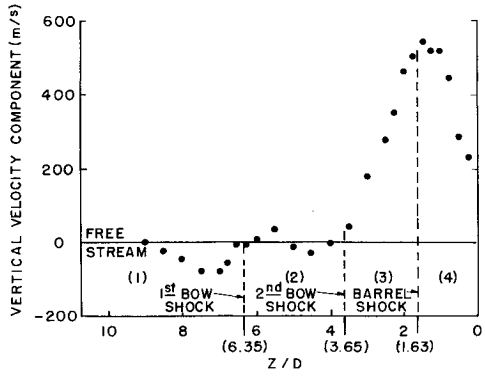

Fig. 14 Measured vertical velocity component distribution along second injector centerline for staged injection with $\bar{q} = 1.20$.

geometry to minimize the background signal level near the wall. These experiments will complete the characterization of the flowfield at more than 500 measurement locations with both staged and single injection at different injection dynamic pressure ratios. A computer-controlled, three-axis, motorized translation system, which will improve the spatial positioning accuracy and ensure repeatability, will be integrated into the experiment. The complete experimental data set will serve as a benchmark for validation of CFD models of a supersonic combustor under nonreacting conditions. This work also provides a foundation for conducting studies of a reacting, hydrogen-fueled, supersonic combustor using laser-induced fluorescence of radical species in the next phase of this research program.

Summary

The spatial resolution and measurement accuracy of a unified, nonintrusive optical technique, LIIF, has been demonstrated in the compressible flowfield of a nonreacting supersonic combustor. The combustor was operated with and without staged, transverse injection behind a rearward-facing step. A measured pressure profile obtained with the calibrated optical technique in the absence of transverse injection agrees very well with both a two-dimensional, method-of-characteristics calculation and a full three-dimensional, Navier-Stokes calculation. Measurements with transverse injection show flow-property discontinuity locations that are in close agreement with shock locations obtained from fluorescence visualization photographs. The sensitivity of the technique to flow property variation and the quantitative nature of the results obtainable from the LIIF technique are evidenced by both experiments.

Acknowledgments

This research was supported by NASA Grant NAG-1-373, Dr. G. Burton Northam, technical monitor. Close interaction with the Hypersonic Propulsion Branch of the Langley Research Center is gratefully acknowledged.

References

[1]Northam, G. B. and Anderson, G. Y., "Supersonic Combustion Ramjet Research at Langley," AIAA Paper 86-0159, Jan. 1986.

[2]Cheng, S., Zimmerman, M., and Miles, R. B., "Supersonic-Nitrogen Flowfield Measurements with the Resonant Doppler Velocimeter," *Applied Physics Letters*, Vol. 43, July 1983, pp. 143-145.

[3]Gross, K. P., McKenzie, R. L., and Logan, P., "Simultaneous Measurements of Temperature, Density, and Pressure in Supersonic Turbulence Using Laser-Induced Fluorescence," NASA TM-88199, Jan. 1986.

[4]McDaniel, J. C. and Hanson, R. K., "Quantitative Planar Visualization in Gaseous Flowfields Using Laser-Induced Fluorescence," *Flow Visualization III*, Hemisphere, Washington, DC, 1985, pp. 113-117.

[5]Cenkner, A. A. and Driscoll, R. J., "Laser-Induced Fluorescence Visualization of Supersonic Mixing Nozzles that Employ Gas-Trips," *AIAA Journal*, Vol. 20, June 1982, pp. 812-819.

[6]McDaniel, J. C. and Graves, J., Jr., "A Laser-Induced Fluorescence Visualization of Transverse, Fuel Injection in a Nonreacting Supersonic Combustor," *Journal of Propulsion and Power*, Vol. 4, Nov.-Dec. 1988, pp. 591-597.

[7]Whitehurst, R. B., "Laser-Induced Fluorescence Flow Visualization of Transverse, Gaseous Fuel Injection into a Supersonic Flow," M. S. Thesis, Univ. of Virginia, Charlottesville, VA, Dec. 1986.

[8]Uenishi, K. and Rogers, R. C., "Three-Dimensional Computation of Mixing of Transverse Injector in a Ducted Supersonic Flow," AIAA Paper 86-1423, June 1986.

[9]McDaniel, J. C., Baganoff, D., and Byer, R. L., "Density Measurement in Compressible Flows Using Off-Resonant Laser-Induced Fluorescence," *Physics of Fluids*, Vol. 25, July 1982, pp. 1105-1107.

[10]McDaniel, J. C., Hiller, B., and Hanson, R. K., "Simultaneous Multiple-Point Velocity Measurements Using Laser-Induced Iodine Fluorescence," *Optics Letters*, Vol. 8, Jan. 1983, pp. 51-53.

[11]McDaniel, J. C.,"Quantitative Measurement of Density and Velocity in Compressible Flows Using Laser-Induced Fluorescence," AIAA Paper 83-0049, Jan. 1983.

[12]Hiller, B. and Hanson, R. K., "Simultaneous Planar Measurements of Velocity and Pressure Fields in Gas Flows Using Laser-Induced Fluorescence," *Applied Optics*, Vol. 27, Jan. 1988, pp. 33-48.

[13]McDaniel, J. C., "Nonintrusive Pressure Measurement with Laser-Induced Iodine Fluorescence," *AIAA Progress in Astronautics*

and Aeronautics: Combustion Diagnostics by Nonintrusive Methods, Vol. 92, edited by T. D. May and J. A. Roux, AIAA, Washington, DC, 1984, pp. 107–131.

[14]Ackermann, U., Baganoff, D., and McDaniel, J. C., "Dependence of Laser-Induced Fluorescence on Gas-Dynamic Fluctuations with Application to Measurements in Unsteady Flow," *Experiments in Fluids,* Vol. 3, March 1985, pp. 1–7.

[15]Nicholson, L. K., "Nonintrusive Pressure Measurement in a Laval Nozzle Using Laser-Induced Iodine Fluorescence," M.S. Thesis, Univ. of Virginia, Charlottesville, VA, Aug. 1985.

[16]Fletcher, D. G. and McDaniel, J. C., "Temperature Measurement in a Compressible Flowfield Using Laser-Induced Iodine Fluorescence," *Optics Letters,* Vol. 12, Jan. 1987, pp. 16–18.

[17]Traving, G., "Interpretation of Line Broadening and Line Shift, *Plasma Dynamics,*" edited by W. Lochte-Holtgreven, North-Holland, Amsterdam, 1978, pp. 66–134.

[18]Uenishi, K., Rogers, R. C., and Northam, G. B., "Three-Dimensional Numerical Predictions of the Flow Behind a Rearward-Facing Step in a Supersonic Combustor," AIAA Paper 87-1962, June, 1987.